

Molecular Structure, Conformation, and Potential to Internal Rotation of 2,6- and 3,5-Difluoronitrobenzene Studied by Gas-Phase Electron Diffraction and Quantum Chemical Calculations

Olga V. Dorofeeva,^{*,†} Anna V. Ferenets,[†] Nikolai M. Karasev,[†] Lev V. Vilkov,[†] and Heinz Oberhammer[‡]

Department of Chemistry, Moscow State University, Moscow 119991, Russia, and Institut für Physikalische and Theoretische Chemie, Universität Tübingen, 72076 Tübingen, Germany

Received: January 31, 2008; Revised Manuscript Received: March 18, 2008

3,5-Difluoronitrobenzene (3,5-DFNB) and 2,6-difluoronitrobenzene (2,6-DFNB) have been studied by gas-phase electron diffraction (GED), MP2 ab initio, and by B3LYP density functional calculations. Refinements of r_{hl} and r_{c} static and r_{hl} dynamic GED models were carried out for both molecules. Equilibrium r_{c} structures were determined using anharmonic vibrational corrections to the internuclear distances ($r_{\text{c}} - r_{\text{a}}$) calculated from B3LYP/cc-pVTZ cubic force fields. 3,5-DFNB possesses a planar structure of C_{2v} symmetry with the following r_{c} values for bond lengths and bond angles: $r(\text{C}-\text{C})_{\text{av}} = 1.378(4) \text{ \AA}$, $r(\text{C}-\text{N}) = 1.489(6) \text{ \AA}$, $r(\text{N}-\text{O}) = 1.217(2) \text{ \AA}$, $r(\text{C}-\text{F}) = 1.347(5) \text{ \AA}$, $\angle \text{C6}-\text{C1}-\text{C2} = 122.6(6)^\circ$, $\angle \text{C1}-\text{C2}-\text{C3} = 117.3(3)^\circ$, $\angle \text{C2}-\text{C3}-\text{C4} = 123.0(3)^\circ$, $\angle \text{C3}-\text{C4}-\text{C5} = 116.9(6)^\circ$, $\angle \text{C}-\text{C}-\text{N} = 118.7(3)^\circ$, $\angle \text{C}-\text{N}-\text{O} = 117.3(4)^\circ$, $\angle \text{O}-\text{N}-\text{O} = 125.5(7)^\circ$, $\angle \text{C}-\text{C}-\text{F} = 118.6(7)^\circ$. The uncertainties in parentheses are three times the standard deviations. As in the case of nitrobenzene, the barrier to internal rotation of the nitro group in 3,5-DFNB, $V_{90} = 10 \pm 4 \text{ kJ/mol}$, is substantially lower than that predicted by quantum chemical calculations. The presence of substituents in the ortho positions force the nitro group to rotate about the C–N bond, out of the plane of the benzene ring. For 2,6-DFNB, a nonplanar structure of C_2 symmetry with a torsional angle of $\varphi(\text{C}-\text{N}) = 53.8(14)^\circ$ and the following r_{c} values for structural parameters was determined by the GED analysis: $r(\text{C}-\text{C})_{\text{av}} = 1.383(5) \text{ \AA}$, $r(\text{C}-\text{N}) = 1.469(7) \text{ \AA}$, $r(\text{N}-\text{O}) = 1.212(2) \text{ \AA}$, $r(\text{C}-\text{F}) = 1.344(4) \text{ \AA}$, $\angle \text{C6}-\text{C1}-\text{C2} = 118.7(5)^\circ$, $\angle \text{C1}-\text{C2}-\text{C3} = 121.2(2)^\circ$, $\angle \text{C2}-\text{C3}-\text{C4} = 119.0(2)^\circ$, $\angle \text{C3}-\text{C4}-\text{C5} = 121.1(4)^\circ$, $\angle \text{C}-\text{C}-\text{N} = 120.6(2)^\circ$, $\angle \text{C}-\text{N}-\text{O} = 115.7(4)^\circ$, $\angle \text{O}-\text{N}-\text{O} = 128.6(7)^\circ$, $\angle \text{C}-\text{C}-\text{F} = 118.7(5)^\circ$. The refinement of a dynamic model led to barriers $V_0 = 16.5 \pm 1.5 \text{ kJ/mol}$ and $V_{90} = 2.2 \pm 0.5 \text{ kJ/mol}$, which are in good agreement with values predicted by B3LYP/6-311++G(d,p) and MP2/cc-pVTZ calculations. The values of C–F bond lengths are similar in both molecules. This is in contrast to the drastic shortening of the C–F bond in the ortho position in 2-fluoronitrobenzene compared to the C–F bond length in the meta and para position in 3- and 4-fluoronitrobenzene observed in an earlier GED study.

1. Introduction

Nitrobenzene and fluorosubstituted nitrobenzenes are of interest since they have different conformational behavior due to the mutual influence through the benzene ring between a nitro group and fluorine atoms in different positions. The structure and dynamic properties of nitrobenzene have been the subject of several experimental and theoretical investigations.^{1–4} This molecule possesses a planar equilibrium structure with a large-amplitude motion around the C–N bond. From experimental microwave spectroscopy (MW) and gas-phase electron diffraction (GED) studies,^{1,4} the barrier to internal rotation was found to be 12.5 and 17.2 kJ/mol, respectively, which is considerably lower than theoretical predictions (19.7–31.4 kJ/mol).⁴

The effect of fluorination of the benzene ring on the structure and dynamic properties has been investigated for 2-, 3-, and 4-fluoronitrobenzene and for 2,4,6-trifluoronitrobenzene.^{5–8} From MW and GED studies,^{5,8} it was shown that 3- and 4-substituted molecules were planar, with the barrier to internal rotation of

17.1 and 14.5 kJ/mol, respectively. Thus, compared to the parent molecule, the substituents in the meta and para positions have practically no effect on the internal rotation of the nitro group. However, the substituents on the benzene ring in the ortho position can force the NO₂ group to rotate out of the plane of the ring. 2-Fluoronitrobenzene was found to be nonplanar, with torsional angles of 32 or 38° determined from MW and GED data,^{5,7} respectively. A substantially larger value of the torsional angle, 57°, was obtained for 2,4,6-trifluoronitrobenzene from an analysis of the MW spectrum.⁵ Unfortunately, the barriers to internal rotation could not be determined from experimental data^{5,7} for the above ortho-substituted molecules. Quantum chemical calculations of the torsional potentials were performed for 2-fluoronitrobenzene and 2,6-difluoronitrobenzene at the MP2/6-31G(d)//HF/6-31G(d) level of theory,⁶ which does not always provide reliable result for such potentials.

In connection with these studies, the structural and dynamical properties of symmetrically fluorinated compounds 3,5-difluoronitrobenzene (3,5-DFNB) and 2,6-difluoronitrobenzene (2,6-DFNB) are of great interest. In the present paper, we report the results of a GED study and MP2 and B3LYP calculations with 6-31(d,p), 6-311++(d,p), and cc-pVTZ basis sets for these two compounds. To determine the torsional potentials for internal

* To whom correspondence should be addressed. E-mail: dorofeeva@phys.chem.msu.ru.

[†] Moscow State University.

[‡] Universität Tübingen.

TABLE 1: Experimental Conditions of the Gas-Phase Electron Diffraction Experiment

	3,5-DFNB		2,6-DFNB	
	long camera	short camera	long camera	short camera
camera distance (mm)	362.28	193.94	362.28	193.94
nozzle temperature (K)	333	333	337	343
accelerating voltage (kV)	60	60	60	60
electron wavelength (Å)	0.049491	0.049186	0.049309	0.049618
number of plates used	3	2	3	3
range of s values (Å ⁻¹) ^a	3.4–18.0	8.0–33.0	3.4–18.0	8.2–32.6
scale factor	0.643(14) ^b	0.619(21)	0.680(16)	0.731(24)

^a Here, $s = 4\pi\lambda^{-1} \sin(\theta/2)$, where θ is the scattering angle and λ is the electron wavelength. ^b Value in parentheses is the estimated standard deviation.

rotation of the nitro group, a dynamic model was applied in the interpretation of GED data. Besides conformation, the change in geometrical parameters due to fluorination is also of considerable interest. From a GED study,⁷ the value of the C–F bond length in 2-fluoronitrobenzene was found to be about 0.03 Å shorter than that in 3- and 4-fluoronitrobenzene.⁸ The observed difference was distinctly larger than that predicted by quantum chemical calculations. The GED investigation of 2,6- and 3,5-DFNB could provide support for this trend of shortening of the C–F bond in ortho positions, while the quantum chemical calculations at a high level of theory could resolve the contradiction between experimental and theoretical results.

2. Experimental Section

Commercial samples of 3,5-DFNB and 2,6-DFNB with purities of 99 and 98%, respectively, were purchased from the Aldrich Chemical Co. and used without further purification. Electron diffraction intensities were recorded using the electron diffraction apparatus at Moscow State University. Details of the experimental conditions are given in Table 1. The electron wavelength was calibrated against diffraction patterns of CCl₄. The optical densities were measured using a commercial Epson Perfection 4870 photo scanner. The data were processed with the program UNEX⁹ using standard routines. The final modified intensity curves are shown in Figures 1 and 2. Numerical values of the experimental intensity curves with the backgrounds are available as Supporting Information (Table S1 and S2 for 3,5- and 2,6-DFNB, respectively). The similarity of the difference curves for the two molecules in the range of 5 Å⁻¹ (Figures 1 and 2) was determined by a small defect of our new sector, which was corrected later. This effect has practically no influence on the final results.

3. Quantum Chemical Calculations

Ab initio MP2 and density functional B3LYP calculations with different basis sets (6-31G(d,p), 6-311++G(d,p), and cc-pVTZ) were carried out to obtain the initial values for geometric and torsional parameters. Potential functions for internal rotation around the C–N bond were obtained by calculating the total energies for torsional angles from 0 to 90° with 10° increments, while all other structural parameters were optimized. To perform the GED refinements, the vibrational amplitudes and vibrational

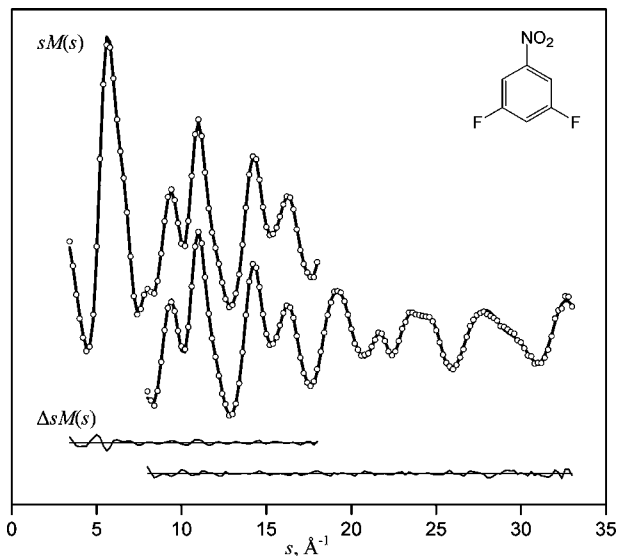


Figure 1. Experimental (open cycles) and theoretical (solid line) molecular intensities $sM(s)$ and the difference curves $\Delta sM(s)$ for the r_e structure model of 3,5-DFNB.

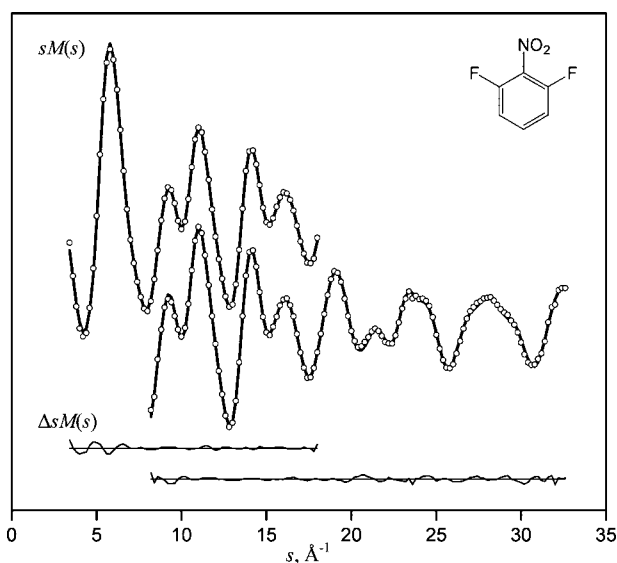


Figure 2. Experimental (open cycles) and theoretical (solid line) molecular intensities $sM(s)$ and the difference curves $\Delta sM(s)$ for the r_e structure model of 2,6-DFNB.

corrections to internuclear distances are also needed, and these were calculated with the harmonic and anharmonic force fields obtained from the B3LYP/cc-pVTZ calculations. All calculations were carried out using the Gaussian 03 program package.¹⁰

3.1. Geometry and Torsional Potential. Computed bond lengths, bond angles, and potential barrier heights for 3,5- and 2,6-DFNB are given in Tables 2 and 3, respectively. Molecular structures of 3,5- and 2,6-DFNB with atom numbering are shown in Figure 3. The torsional potentials for 3,5- and 2,6-DFNB obtained from quantum chemical calculations are given in Figures 4 and 5, respectively. In general, the geometric parameters are not very sensitive to the computational method. Bond lengths agree to within 0.02 Å, and the bond angles differ by no more than 0.9°. It may be noted that the MP2/6-31G(d,p) method predicts rather long N–O bonds.

All calculations for 3,5-DFNB result in planar structures ($\varphi(\text{C–N}) = 0^\circ$), except for the MP2/6-311G++(d,p) method, which predicts a nonplanar structure with torsional angle $\varphi(\text{C–N}) = 15.7^\circ$ and with a small barrier of $V_0 = 0.2$ kJ/mol

TABLE 2: Structural Parameters of 3,5-DFNB Calculated at Different Levels of Theory

parameter ^a	B3LYP			MP2		
	/6-31G(d,p)	/6-311++G(d,p)	/cc-pVTZ	/6-31G(d,p)	/6-311++G(d,p)	/cc-pVTZ
C1–C2	1.392	1.390	1.386	1.392	1.394	1.388
C2–C3	1.389	1.386	1.383	1.390	1.392	1.386
C3–C4	1.392	1.388	1.385	1.391	1.393	1.388
C–N	1.476	1.485	1.481	1.472	1.478	1.471
N–O	1.229	1.223	1.220	1.242	1.231	1.228
C2–H	1.083	1.082	1.079	1.080	1.084	1.079
C4–H	1.081	1.080	1.078	1.078	1.083	1.078
C–F	1.342	1.346	1.341	1.349	1.342	1.336
C6–C1–C2	123.3	123.3	123.2	123.6	123.7	123.4
C1–C2–C3	117.0	116.8	117.0	116.6	116.5	116.8
C2–C3–C4	122.6	122.9	122.7	123.0	123.1	122.8
C3–C4–C5	117.6	117.3	117.5	117.2	117.2	117.5
C–C–N	118.4	118.4	118.4	118.2	118.2	118.3
C–N–O	117.5	117.4	117.4	117.4	117.2	117.3
O–N–O	125.1	125.2	125.2	125.2	125.6	125.5
C1–C2–H	121.3	121.4	121.3	121.7	121.4	121.4
C3–C4–H	121.2	121.3	121.3	121.4	121.8	121.3
C4–C3–F	118.6	118.4	118.5	118.4	118.3	118.5
φ (C2–C1–N–O9)	0	0	0	0	15.7	0
V_0	—	—	—	—	0.2	—
V_{90}	30.1	23.0	23.8	24.0	16.5	21.4

^a Bond lengths are in Å, angles are in degrees, and barriers for internal rotation (V_0 , V_{90}) are in kJ/mol.

TABLE 3: Structural Parameters of 2,6-DFNB Calculated at Different Levels of Theory

parameter ^a	B3LYP			MP2		
	/6-31G(d,p)	/6-311++G(d,p)	/cc-pVTZ	/6-31G(d,p)	/6-311++G(d,p)	/cc-pVTZ
C1–C2	1.400	1.393	1.391	1.394	1.394	1.389
C2–C3	1.389	1.385	1.383	1.389	1.390	1.385
C3–C4	1.395	1.393	1.389	1.396	1.399	1.392
C–N	1.464	1.475	1.471	1.455	1.462	1.456
N–O	1.228	1.220	1.218	1.242	1.231	1.228
C3–H	1.084	1.082	1.080	1.081	1.085	1.079
C4–H	1.085	1.083	1.081	1.082	1.085	1.080
C–F	1.335	1.340	1.334	1.345	1.338	1.333
C6–C1–C2	118.6	118.8	118.8	119.3	119.4	119.4
C1–C2–C3	121.2	121.2	121.1	120.8	121.0	120.9
C2–C3–C4	119.0	118.8	118.9	118.9	118.8	118.9
C3–C4–C5	121.0	121.2	121.1	121.1	121.2	121.1
C–C–N	120.7	120.6	120.6	120.3	120.3	120.3
C–N–O	117.0	116.8	116.8	116.7	116.7	116.6
O–N–O	125.9	126.3	126.3	126.5	126.7	126.8
C3–C4–H	119.5	119.4	119.4	119.4	119.4	119.4
C4–C3–H	122.2	122.0	122.0	122.0	122.0	122.0
C1–C2–F	119.6	119.1	119.3	119.0	118.7	118.9
φ (C2–C1–N–O9)	43.2	59.0	54.2	53.5	66.2	62.6
V_0	7.9	14.2	11.8	16.4	24.6	17.9
V_{90}	7.0	1.8	2.2	3.9	1.8	0.9

^a Bond lengths are in Å, angles are in degrees, and barriers for internal rotation (V_0 , V_{90}) are in kJ/mol.

at the planar configuration. This result, however, has to be considered with caution since it has been demonstrated that the MP2 method with this basis set results in a nonplanar structure for benzene.¹¹ Calculated barriers for perpendicular orientation of the NO₂ group (V_{90}) range between 16.5 and 30 kJ/mol, the lowest value being predicted by the MP2/6-311G++(d,p) method (see Table 2).

According to quantum chemical calculations at different levels of theory (Table 3), 2,6-DFNB possesses a nonplanar equilibrium structure with torsional angles φ (C–N) from 43 to 66°. Except for the B3LYP/6-31G(d,p) method, all theoretical models lead to rather high barriers at the planar configuration (12–25 kJ/mol) and small barriers for orthogonal orientation (1–4 kJ/mol). The B3LYP/6-31G(d,p) method predicts very similar and relatively small barriers of $V_0 = 8$ kJ/mol and $V_{90} = 7$ kJ/mol.

Thus, the quantum chemical calculations give fairly different conclusions about the internal rotation in 3,5- and 2,6-DFNB. The values in Tables 2 and 3 and Figures 4 and 5 demonstrate appreciable differences in torsional angles and barrier heights. For this reason, it is of interest to analyze the GED intensities not only with a static model but also with a dynamic one using different theoretical torsional potentials as starting potential functions. For this purpose, the theoretical energy values were approximated by a Fourier cosine potential

$$V(\varphi) = \frac{1}{2}V_2(1 - \cos 2\varphi) + \frac{1}{2}V_4(1 - \cos 4\varphi) \quad (1)$$

where φ is the torsional angle around the C–N bond. In some instances the use of three potential coefficients V_2 , V_4 , and V_6 led to a somewhat better reproduction of theoretical energy

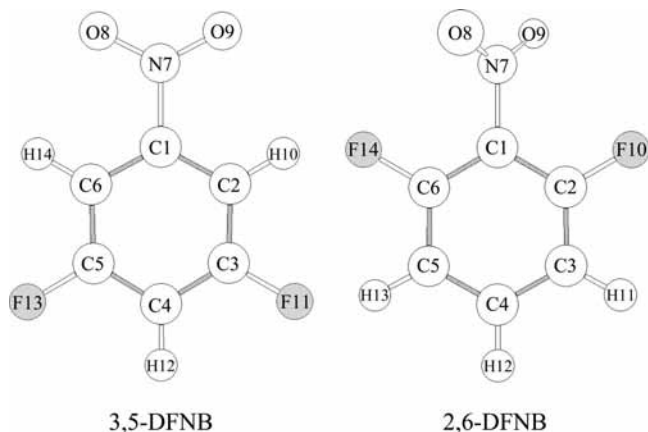


Figure 3. Molecular structures of 3,5-DFNB and 2,6-DFNB with atom numbering.

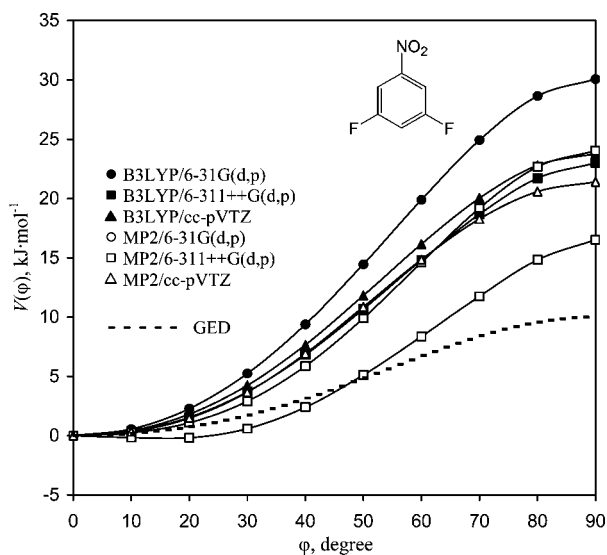


Figure 4. Potential functions for internal rotation around the C–N bond in 3,5-DFNB calculated at the different levels of theory.

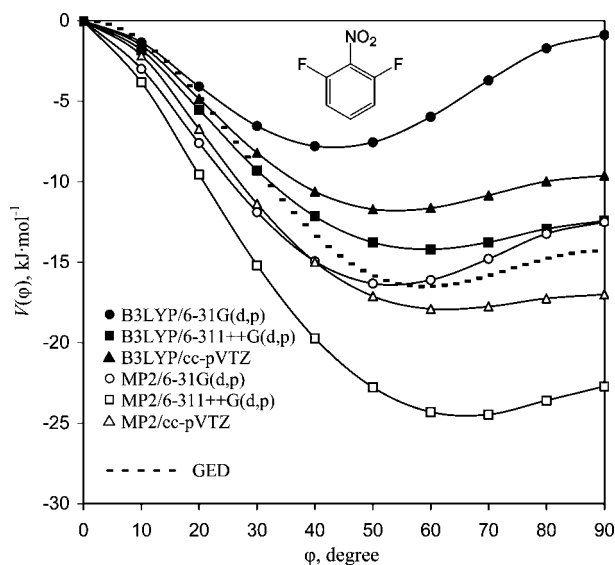


Figure 5. Potential functions for internal rotation around the C–N bond in 2,6-DFNB calculated at the different levels of theory.

values. Attempts to refine three parameters V_2 , V_4 , and V_6 in the GED analysis, however, were not successful. The results of B3LYP/cc-pVTZ calculations were used as the starting values

and constraints for the parameters used in the GED analysis of static and dynamic models.

3.2. Force Field Calculations. In this study, a structural analysis was carried out to obtain an experimental–theoretical approach to the equilibrium r_e geometry by calculating anharmonic vibrational corrections based on the cubic force field. The equilibrium structure, quadratic and cubic force constants, and vibrational frequencies for 3,5- and 2,6-DFNB were calculated at the B3LYP/cc-pVTZ level. The harmonic force constants were calculated from analytical expressions for the second energy derivatives, and the cubic force constants were obtained by numerical differentiation of the second derivatives. From the quadratic and cubic force constants, the amplitudes of vibration (u) and harmonic ($r_{h1} - r_a$) and anharmonic ($r_e - r_a$) vibrational corrections to the internuclear distances were calculated using the SHRINK program.^{12,13} The calculated values of the amplitudes of vibration and the vibrational corrections are given in Table S3 (Supporting Information). These parameters were used as initial values in the GED analysis of static models. For dynamic models, the vibrational amplitudes and harmonic vibrational corrections for each pseudoconformer were also obtained from B3LYP/cc-pVTZ calculations. The vibrational amplitudes were calculated by including the contributions from all normal modes except the torsion about the C–N bond.

The r_e structure determined in this work is one of the possible approximations to the equilibrium geometry. To define accurately the explicit type of structure that has been obtained from a GED experiment, a systematic nomenclature was recently proposed by McCaffrey et al.¹⁴ In accordance with this nomenclature, the equilibrium structure obtained in this work is designated as $r_{a3,1}$.

4. Analysis of the Gas-Phase Electron Diffraction Data

The analysis of GED data was carried out by applying the least-squares method to the molecular intensities using the UNEX program.⁹ In this program, the molecular geometry is specified in a format of a Z-matrix. To keep the symmetry C_{2v} or C_2 for 3,5- and 2,6-DFNB, the interatomic distance $C1 \cdots C4$ was chosen as an independent parameter together with bond lengths and angles given in Table S4 (Supporting Information). Two types of C–C and C–H bonds were refined in groups, with the differences between them constrained to theoretical values. The C–C–H angle was set to the calculated value in all refinements.

Four GED models, namely, the r_a , r_{h1} , and r_e static models and the r_{h1} dynamic model, were analyzed for 3,5-DFNB, and the latter three models were considered for 2,6-DFNB. The determination of starting values for the parameters used in the GED analysis is described in sections 3.1 and 3.2. Vibrational amplitudes were refined in groups. The groups were selected according to the length of the interatomic distances, and the differences within each group were set to calculated values.

To investigate the large-amplitude motion in 3,5- and 2,6-DFNB, a dynamic model was applied in the present GED study. This model is based on the concept that the large-amplitude motion due to torsion of the nitro group can be represented by a mixture of ten pseudoconformers with the dihedral angle $\varphi(C-N)$ ranging from 0 to 90° in steps of 10°. The statistical weight of each pseudoconformer was determined on the basis of its symmetry; the statistical weights of 1 and 2 were used for the C_{2v} ($\varphi = 0$ and 90°) and C_2 ($\varphi = 10$ –80°) forms, respectively. All pseudoconformers were treated as distinct molecules undergoing the usual framework vibrations, except

TABLE 4: Molecular Structure of 3,5- and 2,6-DFNB Obtained by Gas-Phase Electron Diffraction

parameter ^a	3,5-DFNB			2,6-DFNB		
	Static model		Dynamic model	Static model		Dynamic model
	$r_{\text{hl}} (\angle_{\text{hl}})$	$r_{\text{e}} (\angle_{\text{e}})$	$r_{\text{hl}} (\angle_{\text{hl}})$	$r_{\text{hl}} (\angle_{\text{hl}})$	$r_{\text{e}} (\angle_{\text{e}})$	$r_{\text{hl}} (\angle_{\text{hl}})$
C1–C2	1.390(5) ^b	1.380(4) ^b	1.387(4) ^b	1.387(5) ^b	1.379(5) ^b	1.387(5) ^b
C2–C3	1.379(18)	1.375(15)	1.383(15)	1.400(13)	1.392(13)	1.398(13)
C3–C4	1.390 ^b	1.379 ^b	1.386 ^b	1.385 ^b	1.377 ^b	1.387 ^b
C–N	1.500(7)	1.489(6)	1.506(6)	1.480(7)	1.469(7)	1.470(7)
N–O	1.218(2)	1.217(2)	1.215(2)	1.216(2)	1.212(2)	1.215(2)
C–F	1.344(6)	1.347(5)	1.352(4)	1.344(4)	1.344(4)	1.342(4)
C–H ^c	1.097(24) ^e	1.092(25) ^e	1.104(28) ^e	1.076(15) ^e	1.081 ^d	1.081 ^d
C4–H	1.099 ^e	1.093 ^e	1.106 ^e	1.075 ^e	1.080 ^d	1.080 ^d
C6–C1–C2	122.1(6)	122.6(6)	122.9(6)	119.0(4)	118.7(5)	118.6(4)
C1–C2–C3	117.7(3)	117.3(3)	117.1(3)	121.0(2)	121.2(2)	121.2(2)
C2–C3–C4	122.4(3)	123.0(3)	122.8(3)	118.8(2)	119.0(2)	119.0(2)
C3–C4–C5	117.5(6)	116.9(6)	117.2(6)	121.3(4)	121.1(4)	120.9(4)
C–C–N	118.9(3)	118.7(3)	118.6(3)	120.5(2)	120.6(2)	120.7(3)
C–N–O	116.9(4)	117.3(4)	116.9(3)	115.6(4)	115.7(4)	115.7(4)
O–N–O	126.2(8)	125.5(7)	126.2(7)	129.0(7)	128.6(7)	128.6(7)
C–C–F ^f	118.7(8)	118.6(7)	118.6(6)	118.9(5)	118.7(5)	119.2(5)
C–C–H ^g	121.3 ^d	121.3 ^d	121.3 ^d	122.0 ^d	122.0 ^d	122.0 ^d
C3–C4–H	121.2 ^d	121.2 ^d	121.2 ^d	119.4 ^d	119.4 ^d	119.4 ^d
$\varphi(\text{C2–C1–N–O9})$	0.0	0.0	0.0	62.9(13)	53.8(14)	58.8(5)
V_2			10.0(40) ^h			–14.3(3) ⁱ
V_4			–1.0(10) ^h			–7.7(6) ⁱ
R_{L}	4.4	3.5	2.8	4.0	3.4	4.5
R_{S}	5.8	5.6	5.8	4.9	5.5	5.1
R_{tot}	4.8	4.2	3.9	4.3	4.3	4.7

^a Bond lengths are in Å, angles are in degrees, and potential coefficients (V_2 , V_4) are in kJ/mol; values in parentheses are three times the standard deviations. Together with total value of the disagreement factor (R_{tot}), the R factors (in %) are given for long (R_{L}) and short (R_{S}) camera distances. ^b The C1–C2 and C3–C4 bond lengths were refined in the group together with each other, whereas the C1...C4 distance was refined independently (see Table S4 of Supporting Information for adjustable parameters). ^c C2–H for 3,5-DFNB and C3–H for 2,6-DFNB. ^d Theoretical B3LYP/cc-pVTZ values were used in the refinement of GED models. ^e The C4–H bond was refined in the group together with the above C–H bond. ^f C4–C3–F for 3,5-DFNB and C1–C2–F for 2,6-DFNB. ^g C1–C2–H for 3,5-DFNB and C4–C3–H for 2,6-DFNB. ^h The value of $V_{90} = 10$ kJ/mol corresponds to the values of V_2 and V_4 determined by GED. ⁱ The values of $V_0 = 16.5$ kJ/mol and $V_{90} = 2.2$ kJ/mol correspond to the values of V_2 and V_4 determined by GED.

for torsional motion about the C–N bond. The differences in bond lengths, bond angles, and vibrational amplitudes between the planar conformer with $\varphi(\text{C–N}) = 0^\circ$ and other pseudoconformers were taken from quantum chemical calculations. The molecular parameters of the planar conformer were refined in the structural analyses, but the values of other pseudoconformers were deduced by adding the calculated differences to the refined values of the planar conformer. The results of different quantum chemical calculations were used as starting values for the potential coefficients V_2 and V_4 in eq 1. These coefficients were refined in the least-squares procedures in addition to the geometrical parameters from Table S4 (Supporting Information).

4.1. 3,5-Difluoronitrobenzene. Two starting values for the torsional angle, $\varphi(\text{C–N}) = 15.7^\circ$ (MP2/6-311++G(d,p)) and $\varphi(\text{C–N}) = 0^\circ$ (all other theoretical models in Table 2) were used in the GED analysis of static models. A nonplanar structure with $\varphi(\text{C–N}) = 11.5 \pm 7.9^\circ$ was obtained only for the r_{a} model, where vibrational corrections were ignored. Essentially, a planar structure was determined in all GED refinements in which vibrational corrections, both harmonic and anharmonic, were used. The results obtained for the refinement of r_{hl} and r_{e} static models are given in Table 4 (geometrical parameters) and in Table S5 of the Supporting Information (vibrational amplitudes). The resulting radial distribution curve for the r_{e} static model is shown in Figure 6.

The B3LYP/6-31G(d,p) and MP2/6-311++G(d,p) potential functions were used as starting approximations in the dynamic model refinements. As can be seen from Figure 4, these two functions have the highest and the lowest torsional barrier among theoretical potentials calculated in this work. The results

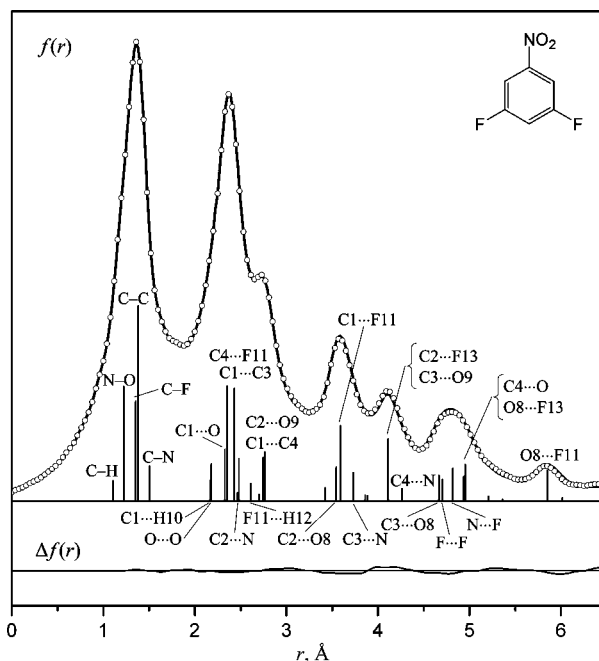


Figure 6. Experimental (open cycles) and theoretical (solid line) radial distribution curves $f(r)$ of 3,5-DFNB with difference curve $\Delta f(r)$ for the r_{e} static model. The distance distribution is indicated by vertical bars.

obtained from the refinements of these two potential functions are shown in Figure 7a and b. The refined GED potential depends on the initial model; however, in both cases, the refined

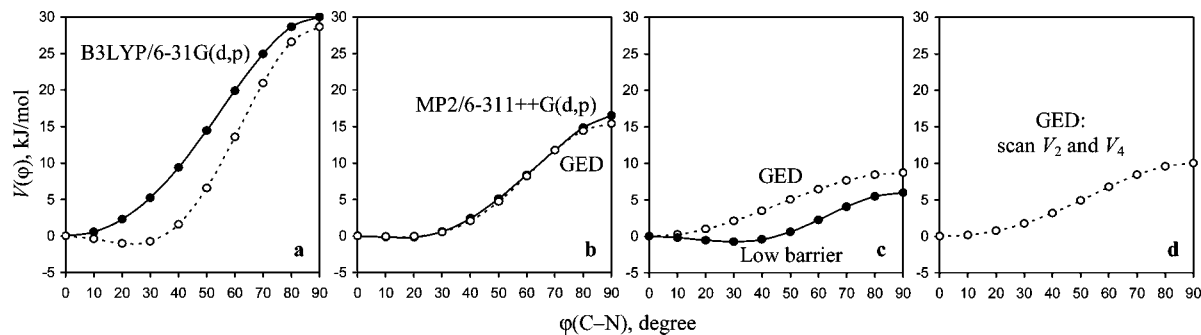


Figure 7. The dynamic model refinements for 3,5-DFNB. The solid line is the initial theoretical potential function, and the dashed line is the result of the GED refinement: (a) B3LYP/6-31G(d,p) theoretical potential, (b) MP2/6-311++G(d,p) theoretical potential, (c) hypothetical potential with low barrier height, and (d) the result of potential coefficients V_2 and V_4 scanning.

value of the V_{90} barrier is lower than the initial guess. Thus, the least-squares procedure can not give an unambiguous solution in this case since the starting values of the V_2 and V_4 coefficients are probably too far from the actual values. These analyses suggest that the actual value of the V_{90} barrier is lower than 15.4 kJ/mol (Figure 7b). To estimate the lowest value of the barrier height, which is in agreement with GED data, a hypothetical potential with a very low barrier of 5 kJ/mol was used as an initial guess (Figure 7c). In this case, the refined value of the barrier (8.7 kJ/mol) was distinctly higher than the starting one, and thus, the GED value of V_{90} lies most likely between those shown in Figures 7b and c, that is, between 8.7 and 15.4 kJ/mol. A more exact estimate of V_{90} was obtained by comparison of R factors for models with different fixed values of V_2 and V_4 . Performing a two-dimensional scan,⁹ models with V_2 values from 5 to 30 kJ/mol and V_4 values from -10 to 10 at 0.5 kJ/mol step were tested. The lowest R factor was obtained for the model with $V_{90} = 10.0$ kJ/mol ($V_2 = 10.0$ kJ/mol and $V_4 = -1.0$ kJ/mol; Figure 7d). This is in agreement with the above conclusion that the resulting GED potential barrier lies between 8.7 and 15.4 kJ/mol. The final GED dynamic model (Table 4) was refined, constraining the V_2 and V_4 coefficients at the values obtained from the scan procedure. The result of group refinement of vibrational amplitudes is given in Table S5 of Supporting Information.

4.2. 2,6-Difluoronitrobenzene. In accordance with theoretical predictions (Table 3), the analysis of the GED data indicates that 2,6-DFNB has a substantially nonplanar structure. The results of the GED analysis of two static and one dynamic model are given in Table 4. The radial distribution curve for the r_e static model is shown in Figure 8. The vibrational amplitudes were refined in the r_{h1} static model only, whereas their values were constrained at theoretical B3LYP/cc-pVTZ values in the r_e static and r_{h1} dynamic model (Table S6 of Supporting Information). The most substantial discrepancy in the resulting parameters of the two static models is observed for the torsional angle; the value obtained for the r_e structure, $\varphi = 53.8^\circ$, is significantly smaller than that for the r_{h1} structure, $\varphi = 62.9^\circ$.

The potential functions given in Figure 5 were used as the initial guesses in the dynamic model analyses. Refinements of all six theoretical potential functions led to potential minima within a narrow range of 58.6 – 59.2° with a mean value of 58.8° . The results of the refinements of four theoretical potential functions are shown in Figure 9. The strongest discrepancy between the starting and refined potential is observed for the B3LYP/6-31G(d,p) model (Figure 9a); the GED data do not support this model with similar values of the V_0 and V_{90} barriers. As shown in Figure 9b and c, the most plausible GED potential lies in the range between the B3LYP/6-311++G(d,p) and MP2/

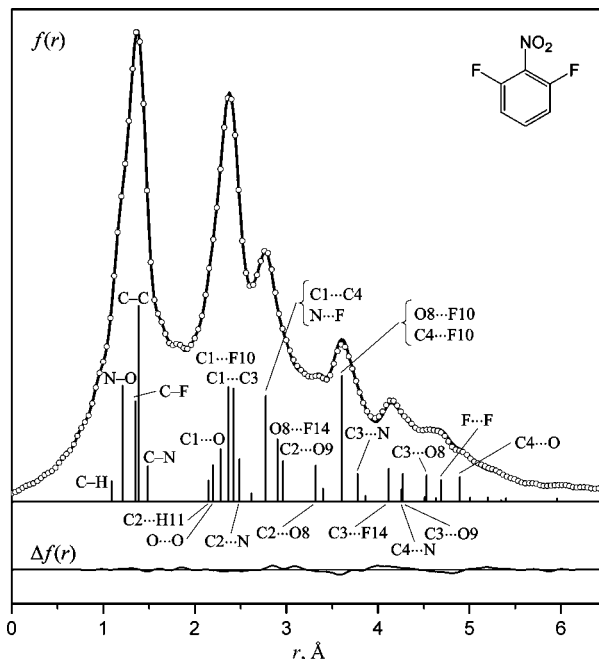


Figure 8. Experimental (open circles) and theoretical (solid line) radial distribution curves $f(r)$ of 2,6-DFNB with difference curve $\Delta f(r)$ for the r_e static model. The distance distribution is indicated by vertical bars.

cc-pVTZ potentials. This suggestion agrees well with the result derived in a V_2 and V_4 scan which led to $\varphi = 57.1^\circ$, $V_0 = 17.3$ kJ/mol, and $V_{90} = 3.0$ kJ/mol ($V_2 = -14.3$ kJ/mol, $V_4 = -8.7$ kJ/mol). The parameters of the dynamic model given in Table 4 were obtained by varying most of the geometrical parameters and the V_2 and V_4 coefficients simultaneously. The resulting GED potential function with $\varphi = 58.8^\circ$, $V_0 = 16.5$ kJ/mol, and $V_{90} = 2.2$ kJ/mol ($V_2 = -14.3$ kJ/mol, $V_4 = -7.7$ kJ/mol) lies between those predicted by B3LYP/6-311++G(d,p) and MP2/cc-pVTZ methods (Figure 5).

5. Results and Discussion

A C_{2v} planar structure was determined to be the equilibrium configuration of 3,5-DFNB, in agreement with results of most quantum chemical calculations. However, the GED value for the torsional barrier, $V_{90} = 10 \pm 4$ kJ/mol, is substantially lower than that predicted by most theoretical calculations (Table 2, Figure 4). For nitrobenzene⁴ as well, theoretical V_{90} barriers are higher than experimental MW and GED values, with the exception of the MP2/6-311++G(d,p) potential, which is in good agreement with the experiments. As is seen from Figure

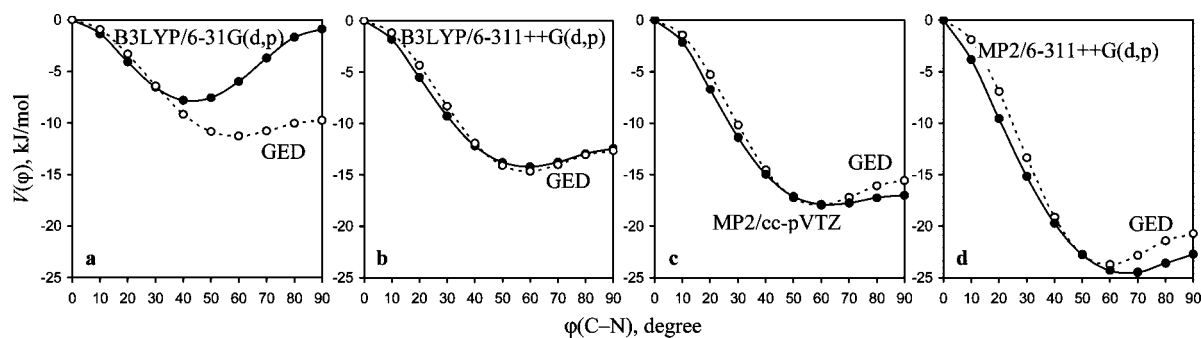


Figure 9. The dynamic model refinements for 2,6-DFNB. The solid line is the initial theoretical potential function: (a) B3LYP/6-31G(d,p), (b) MP2/6-31G(d,p), (c) MP2/cc-pVTZ, and (d) MP2/6-311++G(d,p). The dashed line is the result of the GED refinement.

TABLE 5: Comparison of Structural Parameters of 3,5- and 2,6-DFNB, Nitrobenzene (NB), and 2-, 3-, and 4-Fluoronitrobenzene (FNB) Determined by GED

	3,5-DFNB	2,6-DFNB	2-FNB	3-FNB	4-FNB	NB
parameter ^a	r_e (\angle_e) ^b	r_e (\angle_e) ^b	r_a (\angle_a) ^c	r_g (\angle_g) ^d	r_g (\angle_g) ^d	r_e (\angle_e) ^e
(C–C) _{av}	1.378(5)	1.383(5)	1.395(2)	1.397(4)	1.393(2)	1.391(3)
C–N	1.489(6)	1.469(6)	1.471(13)	1.484(3)	1.479	1.468(5)
N–O	1.217(2)	1.212(2)	1.225(2)	1.227(3)	1.232(3)	1.223(2)
C–F	1.347(5)	1.344(4)	1.306(13)	1.333(8)	1.338(12)	
C6–C1–C2	122.6(6)	118.7(5)	123.8(15)	122.9(24)	120.9(12)	123.5(6)
C1–C2–C3	117.3(3)	121.2(2)	117.5(15)			117.8(5)
C2–C3–C4	123.0(3)	119.0(2)	120.8(12)	119.2(18)		120.3(5)
C3–C4–C5	116.9(6)	121.1(4)			123.8(17)	120.5(6)
C–C–N	118.7(3)	120.6(2)	114.8(10)	118.3(6)	119.1	118.2(3)
C–N–O	117.3(4)	115.7(4)				117.9(2)
O–N–O	125.5(7)	128.6(7)	124.9(8)	125.3(37)	124.2(23)	124.2(4)
C–C–F ^f	118.6(7)	118.7(5)	125.6(18)	120.6(24)		
φ (C–N)	0	53.8(14)	37.6(30)	0	0	0

^a Bond lengths are in Å, and angles are in degrees; the values in parentheses are three times the standard deviations. ^b This work. ^c Ref 7. ^d Ref 8. ^e Ref 4. ^f C4–C3–F for 3,5-DFNB and 3-FNB; C1–C2–F for 2,6-DFNB and 2-FNB.

4, the MP2/6-311++G(d,p) potential is closest to the GED potential in the case of 3,5-DFNB. A refinement of the GED data with the V_2 and V_4 coefficients fixed to the MP2/6-311++G(d,p) values leads to a disagreement factor of $R_{\text{tot}} = 4.3\%$, only slightly higher than that for the final dynamic model ($R_{\text{tot}} = 3.9\%$). Therefore, the GED data do not rule out values of V_{90} for 3,5-DFNB in the range from 10 to 17 kJ/mol.

More accurate information on the torsional potential is obtained for 2,6-DFNB. According to GED data, this molecule is essentially nonplanar, with the torsional angle depending on the GED model. As is seen from Table 4, the use of anharmonic vibrational corrections rather than harmonic ones leads to a significant change in the torsional angle; the value obtained for the r_e static model, $\varphi = 53.8^\circ$, is considerably lower than that for the r_{hl} static model, $\varphi = 62.9^\circ$. The r_{hl} dynamic model results in the value of $\varphi = 58.8^\circ$, and a further decrease of this value is expected when anharmonic vibrational corrections are used. Thus, the value $\varphi_e = 53.8 \pm 1.4^\circ$ most likely provides the best assessment of the torsional angle in 2,6-DFNB. From the discrepancies observed between the starting and refined torsional potentials (Figure 9), it can be concluded that the V_0 barrier is approximately 1 order of magnitude higher than the V_{90} barrier. Therefore, the B3LYP/6-31G(d,p) potential with similar values for both barriers (Table 3) gives an incorrect description for internal rotation in 2,6-DFNB. The values of $V_0 = 16.5 \pm 1.5$ kJ/mol and $V_{90} = 2.2 \pm 0.5$ kJ/mol determined from GED data are in best agreement with those obtained from B3LYP/6-311++G(d,p) and MP2/cc-pVTZ calculations, whereas B3LYP/6-31G(d,p) and MP2/6-311++G(d,p) potential functions (Figure 5) differ most substantially from the GED potential.

The largest discrepancy between experimental and theoretical bond lengths is observed for the C–N distance. The value of r_e (C–N) determined by GED in 3,5-DFNB is 0.004–0.018 Å longer than theoretical values; for 2,6-DFNB, this discrepancy is a little less and does not exceed 0.014 Å. Theory predicts an increase of the C–N bond length in 3,5-DFNB compared to that in 2,6-DFNB by 0.010–0.017 Å, whereas according to GED data, this increase is distinctly larger and ranges from 0.020 to 0.036 Å for the different GED models (Table 4). The GED values of the N–O and C–F bond lengths are similar in both molecules (Table 4) and agree satisfactorily with theoretical values (Tables 2 and 3), with the exception of the overestimated value for r (N–O) predicted by the MP2/6-31G(d,p) method. Among the bond angles, the O–N–O angle in 2,6-DFNB is noteworthy. All theoretical methods predict this angle in 2,6-DFNB to be about 1° larger than that in 3,5-DFNB, whereas this difference varies from 2.4 to 3.2° for GED models, which result in a rather large O–N–O angle ($128.6(7)^\circ$) in 2,6-DFNB.

From comparison of the results of quantum chemical calculations with GED data obtained in this work for 3,5-DFNB and 2,6-DFNB and earlier for nitrobenzene,⁴ one can conclude that the basis set 6-31G(d,p) is inappropriate for nitroaromatic compounds. The MP2/6-31G(d,p) method leads to overestimated N–O bond lengths (Table 2 and 3), whereas the B3LYP/6-31G(d,p) method is poor in reproducing torsional potentials (Figures 4 and 5). Therefore, initial values for geometrical parameters and vibrational amplitudes were taken in this work from B3LYP/cc-pVTZ calculations.

The deformation of the bond angles in the benzene ring is different in the two compounds. The C–C–C angles in 3,5-

DFNB alternate in accordance with Domenicano's rule;¹⁵ the three bond angles at C1, C3, and C5, which are connected to electron acceptor groups NO₂ and F, are larger than 120° (122–123°), whereas the three other angles are about 117°. In 2,6-DFNB, all electron acceptor groups are attached to neighboring carbon atoms in the benzene ring. In this compound, the angles at the carbon atoms bonded to fluorine are larger than 120°, whereas the angle at the carbon atom bonded to the nitro group is smaller than 120°.

A comparison with structural parameters of nitrobenzene and 2-, 3-, and 4-fluoronitrobenzene is given in Table 5. The values for the C–N bond length in molecules with the meta position of fluorine atoms (3,5-DFNB and 3-FNB) is 0.01–0.02 Å longer than those in molecules with an ortho position of fluorine atoms (2,6-DFNB and 2-FNB). On the other hand, it has been demonstrated in the GED studies of 3,5-DFNB and 2,6-DFNB (Table 4) and of nitrobenzene⁴ that the value for this bond length varies within 0.02–0.03 Å, depending on the applied GED model. Since there is an appreciable correlation between the C–N and C–C bonds (Tables S7 and S8 in Supporting Information), the value of the C–N bond length cannot be determined with high precision by GED. Thus, we can not tell with certainty whether the trend in C–N bond lengths upon going from meta- to ortho-fluorinated nitrobenzene is real.

The values for the C–F bonds determined in 3,5-DFNB and 2,6-DFNB (Table 4) are similar to each other and to theoretical values (Tables 2 and 3). This result does not support the drastic shortening of the C–F bond length in the ortho position observed in 2-fluoronitrobenzene as compared to the C–F bond length in the meta and para position in 3- and 4-fluoronitrobenzene^{7,8} (Table 5). It should be noted that GED results for 2-fluoronitrobenzene⁷ differ considerably from theoretical MP2/6-311++G(d,p) values⁷ not only for the C–F bond length ($r(\text{C–F})_{\text{exp}} = 1.306(13)$ Å versus $r(\text{C–F})_{\text{calc}} = 1.337$ Å) but also for some bond angles ($\angle(\text{C6–C1–C2})_{\text{exp}} = 123.8(15)^\circ$ versus $\angle(\text{C6–C1–C2})_{\text{calc}} = 120.8^\circ$, $\angle(\text{C–C–N})_{\text{exp}} = 114.8(10)^\circ$ versus $\angle(\text{C–C–N})_{\text{calc}} = 118.7^\circ$, $\angle(\text{C1–C2–F})_{\text{exp}} = 125.6(18)^\circ$ versus $\angle(\text{C1–C2–F})_{\text{calc}} = 120.4^\circ$). Apparently these data require revision.

Acknowledgment. This research was supported by the Russian Foundation for Basic research under Grant No. 07-03-91557 and by Deutsche Forschungsgemeinschaft under Grant No. DFG 436 RUS 113/69/0-6.

Supporting Information Available: Experimental intensity curves with final backgrounds (Tables S1 and S2), B3LYP/cc-

pVTZ vibrational amplitudes, harmonic and anharmonic vibrational corrections (Table S3), independent geometrical parameters used in structural analysis of 3,5- and 2,6-DFNB (Table S4), experimental and calculated vibrational amplitudes (Tables S5 and S6), and correlation matrixes (Tables S7 and S8). This information is available free of charge via the Internet at <http://pubs.acs.org>.

References and Notes

- (1) Høg, J. H.; Nygaard, L.; Sorensen, G. O. *J. Mol. Struct.* **1970**, *7*, 111.
- (2) Shishkov, I. F.; Sadova, N. I.; Novikov, V. P.; Vilkov, L. V. *Zh. Strukt. Khim.* **1984**, *25*, 98.
- (3) Domenicano, A.; Schultz, G.; Hargittai, I.; Colapietro, M.; Portalone, G.; George, P.; Bock, C. W. *Struct. Chem.* **1990**, *1*, 107.
- (4) Dorofeeva, O. V.; Vishnevskiy, Yu. V.; Vogt, N.; Vogt, J.; Khristenko, L. V.; Krasnoshchekov, S. V.; Shishkov, I. F.; Hargittai, I.; Vilkov, L. V. *Struct. Chem.* **2007**, *18*, 739.
- (5) Correll, T.; Larsen, N. W.; Pedersen, T. *J. Mol. Struct.* **1980**, *65*, 43.
- (6) Staikova, M.; Csizmadia, I. G. *J. Mol. Struct.: THEOCHEM* **1999**, *467*, 181.
- (7) Shishkov, I. F.; Khristenko, L. V.; Vilkov, L. V.; Samdal, S.; Gundersen, S. *Struct. Chem.* **2003**, *14*, 151.
- (8) Shishkov, I. F.; Khristenko, L. V.; Samdal, S.; Gundersen, S.; Volden, H. V.; Vilkov, L. V. *J. Mol. Struct.* **2004**, *693*, 133.
- (9) Vishnevskiy, Yu. V. UNEX: United Nuclear EXperiments. http://molstruct.chemport.ru/mykced_en.html (2007).
- (10) Frisch, M. J.; Trucks, G. W.; Schlegel, H. B.; Scuseria, G. E.; Robb, M. A.; Cheeseman, J. R.; Montgomery, J. A., Jr.; Vreven, T.; Kudin, K. N.; Burant, J. C.; Millam, J. M.; Iyengar, S. S.; Tomasi, J.; Barone, V.; Mennucci, B.; Cossi, M.; Scalmani, G.; Rega, N.; Petersson, G. A.; Nakatsuji, H.; Hada, M.; Ehara, M.; Toyota, K.; Fukuda, R.; Hasegawa, J.; Ishida, M.; Nakajima, T.; Honda, Y.; Kitao, O.; Nakai, H.; Klene, M.; Li, X.; Knox, J. E.; Hratchian, H. P.; Cross, J. B.; Adamo, C.; Jaramillo, J.; Gomperts, R.; Stratmann, R. E.; Yazyev, O.; Austin, A. J.; Cammi, R.; Pomelli, C.; Ochterski, J. W.; Ayala, P. Y.; Morokuma, K.; Voth, G. A.; Salvador, P.; Dannenberg, J. J.; Zakrzewski, V. G.; Dapprich, S.; Daniels, A. D.; Strain, M. C.; Farkas, O.; Malick, D. K.; Rabuck, A. D.; Raghavachari, K.; Foresman, J. B.; Ortiz, J. V.; Cui, Q.; Baboul, A. G.; Clifford, S.; Cioslowski, J.; Stefanov, B. B.; Liu, G.; Liashenko, A.; Piskorz, P.; Komaromi, I.; Martin, R. L.; Fox, D. J.; Keith, T.; Al-Laham, M. A.; Peng, C. Y.; Nanayakkara, A.; Challacombe, M.; Gill, P. M. W.; Johnson, B.; Chen, W.; Wong, M. W.; Gonzalez, C.; Pople, J. A. *Gaussian 03*, revision B.03; Gaussian, Inc.: Pittsburgh, PA, 2003.
- (11) Moran, D.; Simmonett, A. C.; Leach, F. E., III; Allen, W. D.; Schleyer, P. v. R.; Schaeffer, H. F., III *J. Am. Chem. Soc.* **2006**, *128*, 9342.
- (12) Sipachev, V. A. *J. Mol. Struct.: THEOCHEM* **1985**, *121*, 143.
- (13) Sipachev, V. A. *Struct. Chem.* **2000**, *11*, 167.
- (14) McCaffrey, P. D.; Mawhorter, R. J.; Turner, A. R.; Brain, P. T.; Rankin, D. W. H. *J. Phys. Chem. A* **2007**, *111*, 6103.
- (15) Domenicano, A. In *Stereochemical Applications of Gas-Phase Electron Diffraction*, Part B; Hargittai, I., Hargittai, M., Eds.; VCH: New York, 1988, p 281.

JP800941Z